ELSEVIER

Contents lists available at ScienceDirect

Bioresource Technology Reports

journal homepage: www.sciencedirect.com/journal/bioresource-technology-reports





Pilot-scale production of poly-3-hydroxybutyrate-*co*-3-hydroxyvalerate from fermented dairy manure: Process performance, polymer characterization, and scale-up implications

Nicholas M. Guho ^a, Dikshya Pokhrel ^b, Maryam Abbasi ^b, Armando G. McDonald ^b, Maribel Alfaro ^a, Cynthia K. Brinkman ^a, Erik R. Coats ^a, ^{*}

ARTICLE INFO

Keywords: Bioplastic Agricultural waste PHA synthase (phaC) Material properties Resource recovery

ABSTRACT

Polyhydroxyalkanoate (PHA) production from waste feedstocks using mixed microbial consortia (MMCs) is a promising alternative to conventional commercial production from refined feedstocks with axenic cultures. Prior work has reinforced this potential with nutrient-limited waste feedstocks and stringently controlled operation. The process would be more competitive, however, without these restrictions. To that end, a pilot-scale three-stage feast-famine MMC PHA system using dairy manure was operated with relaxed control for 87 days. All three stages absorbed operational fluctuations and exhibited stable performance comparable to tightly controlled analogs. PHA mass fractions (0.29 to 0.40 g/g; volatile solids basis) approached commercial viability and the purified PHA (21 \pm 3% 3-hydroxyvalerate; mole basis) exhibited similarly stable material properties. Finally, characterization of the MMC's PHA synthesizing capability suggested an innate potential for medium-chain-length monomers. Collectively, these results demonstrate the potential for PHA production from a feedstock without a strict nutrient limitation and the process's resilience against operational variability.

1. Introduction

Polyhydroxyalkanoate (PHA) biopolymers represent a potentially renewable alternative to conventional petroleum-based plastics (Sudesh et al., 2000). Synthesized by bacteria on organic substrate, PHAs can be tuned to emulate various forms of petroleum-based plastics, including, but not limited to, polyethylene and polypropylene. Of all bioplastics, this flexibility gives PHA the widest potential for technical substitution in petroleum-based-plastic applications (Shen et al., 2010), making the breadth of the polymer's possible commercial and industrial uses considerable.

Functionally, PHA is an intracellular, amorphous granule synthe-sized by bacteria as a carbon and energy storage reserve (Serafim et al., 2008). However, in a desiccated state PHA, is a biodegradable thermoplastic. Poly-3-hydroxybutyrate (3HB) was the first form of PHA discovered and many additional structures have since been identified (Madison and Huisman, 1999), including poly-3-hydroxyvalerate (3HV) and the copolymer poly-3-hydroxybutyrate-co-3-hydroxyvalerate (PHBV). Carbon substrate dictates structure and polymeric properties

(Madison and Huisman, 1999). PHBV, which is a short chain length PHA of particular interest, is synthesized with even and odd numbered carbon substrate (e.g., acetate and propionate); the polymer exhibits reduced crystallinity and improved ductility relative to 3HB, and is less prone to thermal degradation during processing (Luzier, 1992).

Despite the intrinsic potential of this useful biopolymer, the high production costs of current PHA production methods have impeded broad market penetration and adoption. Conventionally, PHA is produced using synthetic substrate (e.g., refined corn sugar) and pure microbial cultures. While this approach is able to achieve high volumetric productivity and intracellular PHA content, its cost is largely driven by the need to maintain axenic cultures and provide refined carbon substrate (Fernádez-Dacosta et al., 2015). Use of waste substrate can reduce the substrate cost considerably (Bengtsson et al., 2017; Gurieff and Lant, 2007). Additionally, PHA can alternately be synthesized by mixed microbial consortia (MMC) on organic-rich waste substrates (Coats et al., 2016; Dias et al., 2006). Coupling waste-based PHA synthesis with the use of MMC (Dias et al., 2006; Serafim et al., 2008) presents a potentially optimal commercial model within which success can be realized,

E-mail address: ecoats@uidaho.edu (E.R. Coats).

^a Department of Civil and Environmental Engineering, University of Idaho, Moscow, ID, USA

b Department of Forest, Rangeland, and Fire Sciences, University of Idaho, Moscow, ID, USA

^{*} Corresponding author.

particularly considering that many organic-rich waste streams are candidate substrates for the technology. Moreover, diversity of substrates available from waste organics potentially allows production to yield PHAs with tunable material properties.

The most commonly employed strategy for PHA production using MMC and waste substrate is a three-stage system that comprises feedstock fermentation, enrichment of PHA-producing bacteria, and PHA production (Serafim et al., 2008). The fermentation stage converts organic material in waste feedstocks to volatile fatty acids (VFAs; optimal precursors for PHBV synthesis). The enrichment stage is commonly a sequencing batch reactor (SBR) operated under aerobic dynamic feeding (ADF), where the MMC is exposed to short periods of exogenous substrate availability (VFAs) followed by long periods of dearth (Dias et al., 2006; Majone et al., 1996). Under these feast-famine conditions, PHBV-producing bacteria are enriched over non-PHBVproducing bacteria (van Loosdrecht et al., 1997). The production stage then leverages the enriched culture to maximize PHBV production by prolonging exogenous substrate availability. Finally, the PHBV-rich biomass is harvested and subjected to polymer extraction and processing, or can alternately be used to produce composite products (Coats

While the three-stage process has been developed extensively, particularly at bench-scale, several aspects warrant further attention if the potential of PHA production from organic-rich wastes is to be realized at pilot- and full-scale. First, many systems to date have relied on macronutrient limited waste feedstocks to enhance PHA production in the third stage. Second, process stability is commonly ensured through stringent operation with tight control of numerous process parameters. Achieving stable and commercially viable performance without these restrictions would improve the process' competitiveness by expanding the set of amenable feedstocks and reducing operational costs. With an aim to contribute toward future ADF PHBV commercialization, pilotscale research was conducted on a dairy manure-to-PHBV production system with less stringent operational control. The objectives of the investigations were to (i) establish a combined fermenter and PHBV enrichment reactor system (stages 1 and 2) to enrich for an MMC capable of feast-famine PHBV synthesis; (ii) evaluate the PHBV production potential (stage 3) of the enriched culture; (iii) enhance our understanding of the PHBV process through MMC molecular analysis of the PHA synthase gene (phaC); and (iv) characterize the material properties of the PHBV relative to potential commercial applications.

2. Materials and methods

2.1. The PHBV pilot facility and downstream processing

The PHBV pilot facility was designed to produce PHBV-rich biomass from dairy manure using the standard three-stage process (fermentation, enrichment, and production; Serafim et al., 2008). As the names imply, the fermenter fermented the dairy manure to produce a VFA-rich substrate. This substrate was fed to the enrichment reactor (a sequencing batch reactor, SBR) which maintained a PHA-synthesizing MMC. The enriched MMC was then fed the VFA in the enrichment reactor (a sequThe fermenter produced a VFA-rich from the dairy manure, the enrichment reactor (a sequencing batch reactor, SBR) maintained a PHA-synthesizing MMC, and the production reactor (a fed-batch reactor). The data presented herein was collected as part of an 87 d operational period (2019-05-28 to 2019-08-22) at the University of Idaho Dairy Center (Moscow, ID, USA). Over the course of the operational period, the enrichment and production reactors were sampled 15 and 8 times, respectively, to evaluate process performance. Additionally, PHBV-rich biomass produced at the end of each production reactor evaluation was collected for downstream processing and characterization. These sampling events are designated herein by their "operational day" (i.e., the number of days that the enrichment reactor had been operating when the event occurred; see Fig. 1).

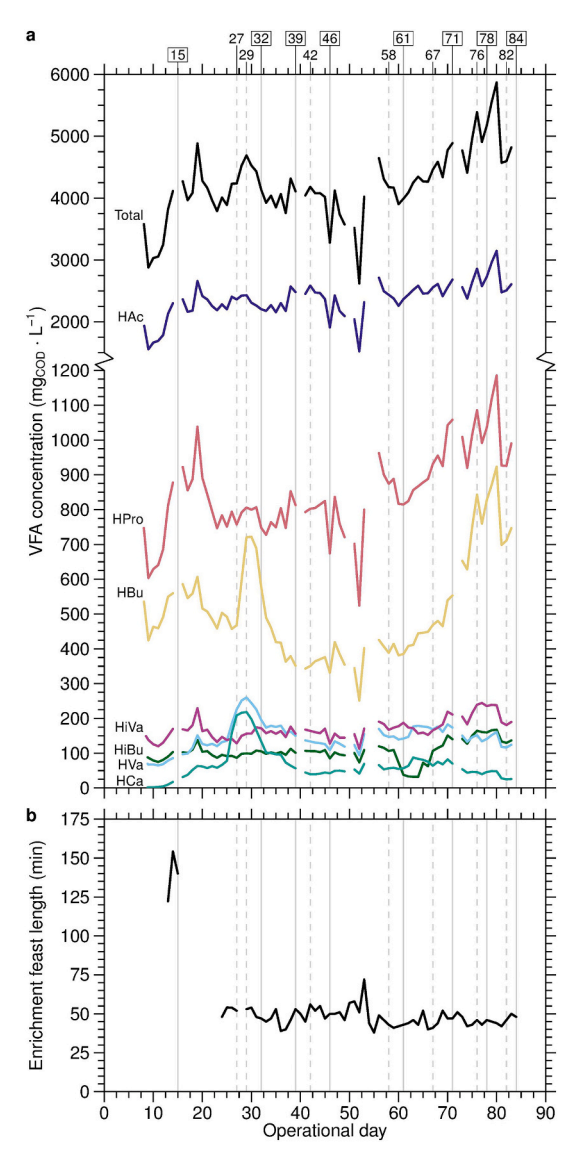


Fig. 1. Routine PHBV pilot monitoring results over the operational period, including the fermenter liquor VFA concentration and speciation (**a**) and the enrichment reactor feast length (**b**). Solid vertical lines denote days on which both the enrichment and production reactors were assessed. Dashed vertical lines denote days on which the enrichment reactor alone was assessed. Note the break and scale change in **a**'s ordinate.

2.1.1. Dairy manure fermenter

The dairy manure fermenter was a 760 L sequencing batch reactor (SBR; baffled with a conical bottom) operated with a theoretical hydraulic residence time (HRT) of 4 d and a cycle length (CL) of 24 h. Each day, 190 L were pumped out of the bottom of the fermenter and, once removed, replaced with an equal volume of homogenized manure (approximately 40 L of freshly collected manure diluted with tap water). The fermenter was continuously mixed with a pitched blade impeller; however, mixing was found to be incomplete. Less dense fibrous materials aggregated in a layer near the surface, while more dense materials (e.g., rocks and seeds) remained near the bottom. Recognizing that this heterogeneity greatly complicates its accurate quantification, the solids retention time (SRT) of the system was estimated to be 4 d by crudely idealizing the fermenter as completely mixed. Temperature was neither controlled nor monitored. The ambient temperature ranged from approximately 4 to 36 °C over the operational period (www.ncdc.noaa. gov); however, the reactor's mass and its location in an enclosure modulated the in-reactor range (Section 3.2).

The substrate for the second and third stages of the process was recovered daily from the fermenter effluent through a three-step process aimed at removing the suspended solids. First, the fermenter effluent was passed through a stainless steel mesh screen (0.5 mm opening) to remove large particles. The recovered liquid was then pumped at 6 to 7 L/min through a drum centrifuge (1220·g; Model SUS304, US Filtermaxx, Green Cove Springs, FL, USA). Finally, the centrate was filtered through 10 μm nylon mesh sock filters (Duda Energy LLC, Decatur, AL, USA). The filtrate—termed the "fermenter liquor"—was then stored under ambient conditions for subsequent use in the enrichment and production reactors. As the fermenter was undersized relative to the enrichment and production reactors, the excess fermenter liquor (i.e., that leftover after satisfying enrichment reactor operation) was accumulated for 3 to 5 d prior to production assessments.

2.1.2. Enrichment reactor

The enrichment reactor was a 680 L, baffled, conical-bottom tank inoculated with 38 L of return activated sludge from the City of Moscow Water Reclamation and Reuse Facility (Moscow, ID, USA). The reactor was operated manually as an SBR with a CL of 24 h (SRT and HRT of 4 d) and was fed fermenter liquor diluted with an equal volume of tap water. Each cycle consisted of a fill phase (10 to 12 min) during which the diluted fermenter liquor was fed to the reactor, followed by a react phase, and ending with a waste phase (10 to 20 min). Continuous mixing and aeration was achieved with a pitched blade impeller and a rotary lobe blower (Roots 24 URAI; Howden Group, Renfrew, UK) which delivered air through an array of eight fine bubble diffusors (Sanitaire Silver Series, 9 in diameter, Xylem Inc., Rye Brook, NY, USA). The air flowrate was monitored (280 to 350 L/min), but not controlled. The dissolved oxygen concentration (C_{DO}) was monitored intermittently during the first 28 d of operation using a Hach HQ40d meter with an LDO101 probe and online thereafter using a Hach sc200 controller with an LDO2 probe (Hach Company, Loveland, CO, USA). ORP was measured with a Hach MTC101 or MTC301 probe and HQ40d meter. pH was measured with a Hach PHC301 probe and HQ40d meter, but not controlled. Temperature was monitored, but not controlled.

2.1.3. Production Reactor

The ability of the MMC enriched in the enrichment reactor to produce PHBV was assessed eight times over the operational period by subjecting the consortium to repeated "feast" phases without interceding "famine" phases. The production assessments were fed-batch where the waste from that day's enrichment reactor cycle (the enriched MMC) was fed multiple pulses of fermenter liquor to maximize PHA production. Assessments were conducted in a 450 L, baffled, conical-bottom tank that was continuously mixed with a pitched blade impeller. The production reactor was aerated with a diffusor array identical to the enrichment reactor's that was fed by the same rotary lobe blower. The aeration rate was monitored (100 to 200 L/min) and controlled manually to maintain aerobic conditions during production assessments. C_{DO} was recorded with a handheld meter (Hach LDO101 probe with an HQ40d meter) for the first production assessment and online thereafter (Hach LDO2 probe and sc200 controller). ORP was measured with a Hach MTC101 or MTC301 probe and HQ40d meter. pH was measured with a Hach PHC301 probe and HQ40d meter, but not controlled. Temperature was monitored, but not controlled.

At the start of each assessment, the enriched MMC was supplemented with tap water to bring the initial volume to approximately 210 L. This dilution was necessary to achieve adequate mixing and aeration from the assessment's outset. Three to seven pulses of fermenter liquor were fed to the reactor during each assessment; volumes supplied were determined to achieve a maximum VFA concentration in the reactor on par with that realized in the enrichment reactor. After the initial pulse, subsequent pulses were added based on the $C_{\rm DO}$ (Dias et al., 2006; Serafim et al., 2004). Once the $C_{\rm DO}$ spiked after the addition of the last pulse, the production reactor's air was shut off and its contents

centrifuged (pumped at 6 to 7 L/min through the same drum centrifuge used in fermenter effluent processing). Once centrifugation was complete, the separated solids (i.e., the PHBV-rich biomass) were recovered, divided into samples (each approximately 1 kg), massed, and frozen. Supplemental stressors (e.g., an outright macronutrient limitation; see Section 3.1) were not imposed on the MMC to enhance productivity.

2.1.4. PHBV-rich biomass downstream processing

PHBV was recovered from the PHBV-rich biomass produced at the PHBV pilot facility following extraction and purification. A portion of each batch of frozen PHBV-rich biomass (1 to 2 kg) was lyophilized and then washed four times with acetone to remove lipids. In each washing, the biomass was constantly stirred for 24 h in acetone (4 L for the first, 1 L thereafter) and then recovered by vacuum filtration. After the final washing, the acetone-washed PHBV-rich biomass was air dried, yielding 150 to 260 g. The crude PHBV was extracted from the acetone-washed PHBV-rich biomass in chloroform (3.5 L) using a Soxhlet extractor and recovered by concentration to dryness in a rotary evaporator. The crude PHBV (30 to 58 g) was then purified by two non-solvent precipitations. First, the crude PHBV was redissolved in chloroform (100 mL) and then added dropwise to cold, constantly stirred petroleum ether (4 °C, 1.5 L) to precipitate the PHA. After recovery by filtration and air drying, the PHA was redissolved in chloroform (100 mL) and added dropwise to cold, constantly stirred methanol (4 °C, 1.5 L), which precipitated the purified PHBV. Finally, the purified PHBV was recovered by filtration and dried under vacuum.

2.2. Analyses

2.2.1. Chemical analyses

Samples were collected to monitor ammonia (NH₃), VFAs, reactive phosphorus (PO $_4^{-3}$), total solids (TS), volatile solids (VS), total suspended solids (TSS), volatile suspended solids (VSS), and PHBV. For soluble constituents, samples were first centrifuged to remove biomass, then filtered through a 0.22 μ m syringe filter (Pall Corporation, Port Washington, NY, USA), and stored on ice prior to testing. Soluble NH₃ and PO $_4^{-3}$ concentrations were determined in accordance with Hach methods 10031 and 8048, respectively (both consistent with Standard Methods; Anonymous, 2012) each utilizing a linear standard curve ($R^2 > 0.99$). TS, VS, TSS, and VSS were measured in accordance with Standard Methods (Rice et al., 2012).

2.2.2. VFA by gas chromatography/flame ionization detection

VFAs (acetic, propionic, butyric, isobutyric, valeric, isovaleric, and caproic acids) were quantified using a Hewlett-Packard 6890 series gas chromatograph (GC) equipped with a flame-ionization detector (FID) and a 7679 series injector (Agilent Technologies, Inc., Santa Clara, CA, USA). The system was interfaced with the Hewlett-Packard GC Chem-Station software (version A.06.01; Agilent Technologies, Inc.). VFA separation was achieved using a capillary column (Zebron ZB-Waxplus, 30 m, 0.25 mm ID; Phenomenex Inc., Torrance, CA, USA) subjected to the following temperature program: (i) hold at 50 °C for 2 min, (ii) increase to 95 °C at 30 °C/min, (iii) increase to 150 °C at 10 °C/min, (iv) hold at 150 °C for 3 min, (v) increase to 200 °C at 25 °C/min, and (vi) hold at 200 °C for 12 min. Helium was used for the carrier gas (1.2 mL/ min). The injector and detector were operated isothermally at 210 $^{\circ}\text{C}$ and 300 °C, respectively. Prior to analysis, samples were acidified to a pH of 2 using nitric acid. 0.5 µL of each sample was injected in 20:1 split mode. VFA concentrations were determined through retention time matching with known standards (Sigma-Aldrich Co., St. Louis, MO, USA; Thermo Fisher Scientific Inc., Waltham, MA, USA) and linear standard curves $(R^2 > 0.99)$.

2.2.3. PHBV by gas chromatography/mass spectrometry

The PHBV content of biomass samples was determined by gas chromatography/mass spectrometry (GC–MS). Enrichment and

production assessment biomass samples (10 mL) were preserved with 100 µL bleach, stored on ice, centrifuged (5 min at 2400g), drained, rinsed with deionized water, and dried at 105 °C. After massing, biomass samples (20 to 40 mg) were digested for 4 h at 100 $^{\circ}$ C in 4 mL of a 1:1 (ν / v) mixture of acidified methanol (3%H2SO4; v/v) and chloroform (with 0.25 to 0.5 mg/mL benzoic acid; an internal standard). After digestion and cooling, the solution was separated into organic and aqueous phases with the addition of 1 to 2 mL of deionized water followed by vortex mixing. The organic phase was then extracted and filtered through a small column of anhydrous Na2SO4 (to remove excess moisture and particulates) into a GC vial. GC-MS was performed on an ISQ7000-Trace1300 GC-MS system (Thermo Fisher Scientific Inc.). Separation was achieved on a capillary column (ZB1, 30 m, 0.25 mm ID; Phenomenex Inc.) with helium as the carrier gas (1.2 mL/min) and an initial temperature of 40 °C (held for 2 min) ramped to 200 °C at 5 °C/min. 3HB and 3HV were quantified relative to the internal standard from known standards (0.12 to 0.21 mol_{3HV}/mol_{PHBV}; Sigma-Aldrich Co.; TianAn Biologic Materials Co., Ltd., Ningbo, People's Republic of China), as confirmed by retention time and mass spectral matching; the optimal ion for quantification was determined to be m/z = 103 for both monomers. Additionally, two degradation products generated during the methanolysis of PHBV were similarly quantified and included in the final 3HB and 3HV quantities: methyl-2-butenoic acid (from 3HB, quantified by ion m/z = 100) and methyl-2-pentenoic acid (from 3HV, quantified by ion m/z = 114), both prepared from known standards (Alfa Aesar, Haverhill, MA, USA; Acros Organics, Geel, Belgium). The Xcalibur software program (v4.1.31.9; Thermo Fisher Scientific Inc.), MSFileReader (v3.0 sp1; Thermo Fisher Scientific Inc.), and the Thermo Raw File Reader (Pacific Northwest National Laboratory, https://omics. pnl.gov/software/thermo-raw-file-reader) were used for PHBV quantification.

2.2.4. Size exclusion chromatography (SEC)

The number- and weight-average molecular weights $(\overline{M_n} \text{ and } \overline{M_w})$ of PHBV were determined by size exclusion chromatography (SEC). A Jordi DVB linear mixed bed column (300 mm, 7.8 mm ID; JordiLabs, LLC, Mansfield, MA, USA) was used for the separation of PHBV at 30 °C. PHBV samples (100 μ L, 2 mg/mL) were filtered (0.45 μ m, PTFE), injected on elution with chloroform at 0.5 mL/min and detected with a Waters model 2414 refractive index detector (Waters Corporation, Milford, MA, USA) and a PostNova PN3609 (658 nm) multi-angle light scattering (MALS) detector (Postnova Analytics GmbH, Landsberg am Lech, Germany). A refractive index increment (d_n/d_c) value of 0.034 for 3HB in CHCl₃ was used (Negulescu et al., 2008). Data were analyzed using the NovaSEC v1.5.0 software (Postnova Analytics GmbH). The system was calibrated using a narrow polystyrene standard ($M_w = 105,268$ g/mol; Malvern Panalytical Ltd., Malvern, United Kingdom).

2.2.5. Differential scanning calorimetry (DSC)

PHBV samples (4 to 6 mg, in triplicate) and 0.21 $\mathrm{mol}_{\mathrm{3HV}}/\mathrm{mol}_{\mathrm{PHBV}}$ standard (TianAn Biologic Materials Co., Ltd.) were analyzed on a Q200 DSC with refrigerated cooling (TA Instruments, New Castle, DE, USA) using the following regime: equilibrated at 40 °C (3 min) then (i) ramped at 10 °C/min to 180 °C (3 min) to remove any prethermal history, (ii) cooled at -10 °C/min to -50 °C (held for 3 min), and (iii) the cycle repeated. The melt temperature (T_{m}) and the glass transition temperature (T_{g}) were determined from the peak maximum and the inflection point of the second heating scan, respectively. The degree of crystallization (X_{c}) of samples were calculated from the ratio of the melting enthalpy (δH_{f}) of the sample to melting enthalpy (δH_{f}) of 100% crystalline 3HB (146 J/g for PHBV; Berthet et al., 2015). Data were analyzed using TA Universal analysis v4.5A software (TA Instruments).

2.2.6. NMR spectroscopy

¹H NMR spectroscopy was performed on purified PHBV samples and

the $0.21~{\rm mol_{3HV}/mol_{PHBV}}$ standard (TianAn Biologic Materials Co., Ltd.) dissolved in CDCl₃ using a 300 MHz Bruker spectrometer (Bruker Corporation, Billerica, MA, USA). Spectra were analyzed using TopSpin v3.6.2 software (Bruker Corporation). The 3HV to 3HB molar fraction was determined using the ratio of the integrated $^1{\rm H}$ peak areas due to the 3HV methyl resonance and the sum of 3HB + 3HV methyl resonance (Wei et al., 2014).

2.2.7. Quantitative polymerase chain reaction (qPCR)

qPCR was performed on genomic DNA recovered from the enrichment reactor on six operational days (58, 61, 67, 71, 78, and 84) to estimate the abundance of class I, II, III, and IV phaC genes relative to the total eubacterial population. Genomic DNA was extracted using the MO BIO PowerSoil DNA Isolation Kit (Qiagen, Hilden, Germany). Genomic DNA yield and purity was quantified using a NanoDrop ND-1000 Spectrophotometer (Thermo Fisher Scientific Inc.). The primer sets used to quantify the total bacteria and phaC gene classes I, II, III, and IV abundances are summarized in Table S1. Amplification and quantification were achieved with an Applied Biosystems Step-one-plus qPCR system (Thermo Fisher Scientific Inc.); qPCR settings and estimation of phaC gene relative abundance in the bacterial population were in accordance with Winkler et al. (2011). Replicate qPCR was performed for all samples on a given 96 well plate. qPCR melting curves were evaluated to confirm a single melting peak; agarose gel analysis confirmed a single band for each primer set. Amplification efficiencies were calculated for each primer set using baseline-corrected fluorescence data (StepOne software v2.3, Thermo Fisher Scientific Inc.) and the LinRegPCR program (Ramakers et al., 2003). The cycle threshold was set at a constant value of 0.2 within the log-linear region across all samples for determination of quantification cycle values.

2.3. Calculations

The PHBV mass fraction (fPHBV) was quantified differently for inreactor and PHBV-rich biomass samples. For samples taken from the enrichment and production reactors during the assessments, TSS and VSS concentrations (C_{TSS} and C_{VSS} , respectively) were not always available at the same time as the maximum PHBV concentration (due to different sampling frequency). Additionally, the C_{TSS} and C_{VSS} were variable (a product of the high solids concentration and the associated difficulty in collecting and processing representative samples). As such, the in-reactor PHBV mass fraction estimates are expressed on a centrifuged solids (CS) basis (i.e., $f_{PHBV,CS}$) where the CS was quantified as part of the PHBV assay. In contrast, the PHBV fraction in the PHBV-rich biomass was quantified on a TS or VS basis (i.e., $f_{PHBV,TS}$ and $f_{PHBV,VS}$, respectively) where appropriate. For similar reasons, the active biomass concentration (C_X) was estimated as the centrifuged solids concentration less the PHBV concentration (i.e., $C_{\rm X}=C_{\rm CS}-C_{\rm PHBV}$). Finally, the stoichiometric and kinetic process variables of interest were estimated using univariate linear regression of the corresponding concentrations.

3. Results and discussion

3.1. Dairy manure fermenter

Dairy manure fermentation has been shown to be a reliable and consistent means of generating VFAs, particularly at bench-scale where key operating parameters—like the organic loading rate (OLR; $g_{VS}/(L\cdot d)$) and mixing regime—can be tightly controlled (Coats et al., 2012; Stowe et al., 2015). Recognizing that such strict control may not be feasible at full-scale, the dairy manure fermenter operated in this study was fed volumetrically (with the OLR being allowed to fluctuate with changes in manure composition) and mixed imperfectly. Despite the lack of explicit OLR control, the TS and VS entering the fermenter were generally consistent (3.40 \pm 0.38% and 2.72 \pm 0.32%, respectively; mean \pm standard deviation; n=12). This resulted in an OLR to the

fermenter of 6.8 \pm 0.8 $g_{VS}/(L\cdot d).$ While the *OLR* magnitude was lower than prior bench-scale investigations (typically approximately 9 $g_{VS}/$ (L·d)), the less stringent fermenter control exerted herein did not induce significant variability.

As expected with a lower OLR, effluent TS and VS were lower than at bench-scale (3.19 \pm 0.66%, n=12 vs. 3.7% and 2.53 \pm 0.61%, n=12 vs. 3.0%, respectively); however, the mean VS reduction, while variable, was in the range previously observed (5.7% vs. 3.2 to 16.8%, Coats et al., 2012; Stowe et al., 2015). The variability observed in the pilot fermenter's effluent solids may be attributed, at least in part, to vertical stratification and suboptimal sample collection (single grab samples of the non-homogenized effluent). Nevertheless, at the scale considered herein, the incomplete mixing does not appear to have been overly detrimental to the fermenter's performance, at least in terms of solids reduction.

Despite the less stringent control exerted over the OLR, both the total VFA concentration and odd-carbon-chain-length VFA fraction in the fermenter liquor were generally consistent (4200 \pm 600 mg_{COD,VFA}/L and 0.28 \pm 0.01 mg_{COD,Odd}/mg_{COD,VFA}, respectively, n=70; Fig. 1a). Both were low relative to bench-scale results (5100 to 7200 mg_{VFA,COD}/L and 0.32 to 0.34 mg_{COD,Odd}/mg_{COD,VFA} Coats et al., 2016; Hanson et al., 2016) which hampered the overall volumetric productivity and ultimately resulted in lower 3HV fractions (Section 3.5 and Tables 1 and 3). While the low total VFA concentration may be attributed, at least in part, to the low OLR, the root cause of the suboptimal odd-carbon-chain-

Table 1 Enrichment reactor assessment summary. a

Operational day	$C_{\rm X}^{\ \ m b}$	$q^{\max}_{\text{VFA}}^{\text{b}}$	Y ^{obs} _{PHBV,VFA} ^b	$f_{ m PHBV,}$	$f_{ m 3HV,PHBV}^{ m d}$	
	g _X /L	g _{COD,VFA} / (g _X ·h)	8COD,PHBV/ 8COD,VFA	g _{PHBV} / g _{CS}	mol _{3HV} / mol _{PHBV}	
15	$\begin{array}{c} 2.0 \pm \\ 0.1 \end{array}$	$\begin{array}{c} \textbf{0.11} \pm \\ \textbf{0.01} \end{array}$	0.72 ± 0.06	0.088	0.18	
27	$\begin{array}{c} \textbf{2.1} \pm \\ \textbf{0.1} \end{array}$	$\begin{array}{c} 0.25 \pm \\ 0.01 \end{array}$	1.0 ± 0.2	0.106	0.22	
29	$\begin{array}{c} 2.5 \pm \\ 0.1 \end{array}$	$\begin{array}{c} \textbf{0.22} \pm \\ \textbf{0.01} \end{array}$	0.9 ± 0.2	0.100	0.23	
32	$\begin{array}{c} \textbf{2.6} \pm \\ \textbf{0.1} \end{array}$	$\begin{array}{c} 0.25 \pm \\ 0.02 \end{array}$	$\textbf{0.77} \pm \textbf{0.08}$	0.099	0.24	
39	$\begin{array}{c} \textbf{2.4} \pm \\ \textbf{0.1} \end{array}$	$\begin{array}{c} 0.23 \pm \\ 0.02 \end{array}$	0.65 ± 0.06	0.091	0.25	
42	$\begin{array}{c} \textbf{2.2} \pm \\ \textbf{0.1} \end{array}$	$\begin{array}{c} 0.30 \pm \\ 0.01 \end{array}$	$\textbf{0.68} \pm \textbf{0.05}$	0.108	0.27	
46	2.3 ± 0.1	0.29 ± 0.02	0.66 ± 0.05	0.096	0.28	
58	2.9 ± 0.1	0.25 ± 0.02	$\textbf{0.87} \pm \textbf{0.08}$	0.087	0.31	
61	2.8 ± 0.1	0.24 ± 0.01	$\textbf{0.97} \pm \textbf{0.03}$	0.087	0.32	
67	2.3 ± 0.1	0.44 ± 0.02	0.73 ± 0.05	0.104	0.31	
71	$\begin{array}{c} {\bf 2.4} \pm \\ {\bf 0.1} \\ {\bf 2.5} \pm \end{array}$	$\begin{array}{c} \textbf{0.35} \pm \\ \textbf{0.01} \end{array}$	0.80 ± 0.06	0.116	0.35	
76	2.5 ± 0.1 2.7 ±	0.4 ± 0.1 $0.39 \pm$	0.7 ± 0.2	0.110	0.30	
78	0.1 2.4 ±	0.03 0.32 ±	0.54 ± 0.05	0.096	0.28	
82	0.1 2.7 ±	0.01 0.28 ±	0.89 ± 0.04	0.103	0.27	
84	0.1	0.20 ±	0.67 ± 0.03	0.085	0.26	

^a Symbols are define as: $C_{\rm X}$ is the active biomass concentration; $q^{\rm max}_{\rm VFA}$ is the maximum specific VFA uptake rate; $Y^{\rm obs}_{\rm PHBV,VFA}$ is the observed yield of PHBV on VFA; $f_{\rm PHBV,CS}$ is the PHBV mass fraction of the centrifuged solids; and $f_{\rm 3HV,PHBV}$ is the 3 HV fraction of the PHBV.

length VFA fraction could not be definitively identified.

VFAs were not the only potential substrate in the fermenter liquor. Spot checks suggested that the VFAs constituted 38 to 58% of the sCOD, which is lower than has been observed previously at bench-scale (71%; Hanson et al., 2016) and in comparable pilot-scale systems (53 to 91%; Conca et al., 2020; Tamis et al., 2014, 2018; Valentino et al., 2018, 2019). Considering the PHA production process in total, a high relative VFA fraction is necessary to maximize overall efficiency; higher VFA production in the fermenter translates to higher PHA production overall. A high relative VFA fraction in the fermenter liquor can also bolster the enrichment reactor's performance by reducing the non-VFA sCOD that may support non-PHBV producing bacteria (Jiang et al., 2012). While the comparatively low VFA fraction undermined overall productivity (Section 3.6), its impact on the enrichment reactor specifically was likely lessened by the non-VFA sCOD's availability. Spot checks of the enrichment reactor effluent revealed a significant residual sCOD concentration (1000 to 1500 mg_{sCOD}/L), suggesting that at least a portion of the non-VFA sCOD in the fermenter liquor (possibly upwards of 32%) was not consumed and thus did not contribute to supporting a non-PHBV population. Discounting this residual concentration from the non-VFA sCOD, the VFA fraction of the sCOD may have been as high as 70%.

Macronutrients (in particular N, P) are also critical to PHBV production. Prior work with dairy-manure-derived fermenter liquor has suggested that it, like many excreta-sourced waste streams, is neither N-nor P-limited (Coats et al., 2016). Spot checks of C_{NH3} supported this conclusion (537 to 662 mg_{N,NH3}/L was observed, yielding a mean C/N ratio of 2.9 mol_{C,VFA}/mol_{N,NH3}); however, similar checks of C_{P04}^{O3} suggest that the fermenter liquor may have been dual C- and P-limited (33.4 to 43.4 mg_{P,PO4-3}/L was observed, yielding a mean C/P ratio of 100 mol_{C,VFA}/mol_{P,PO4}). This nutrient deficiency bodes well for the three-stage PHBV process as a treatment technology in light of the environmental challenges facing dairies. However, in the context of PHBV production specifically, the implications of this dual limitation are minor (comparable performance has been reported for C-limited and dual C- and P-limited three-stage PHBV systems; Korkakaki et al., 2017).

Whereas the VFAs, non-VFA COD, and macronutrient concentrations were suitable for PHBV production, the fermenter liquor's suspended solids concentration posed significant challenges. Despite the solids reduction operations employed, the fermenter liquor's $C_{\rm TSS}$ and $C_{\rm VSS}$ ranged from 2.3 to 8.8 g_{TSS}/L and 2.1 to 6.6 g_{VSS}/L, respectively. Though this is a another difficulty attending the use of waste feedstocks for PHBV production, it is not insurmountable. Alternative solids separation approaches have proven successful for other waste feedstocks (e.g., filter pressing and coagulation-flocculation), albeit at a higher cost.

3.2. Enrichment reactor

The enrichment reactor's *SRT*, *HRT*, *CL*, and *OLR* were adopted from successful bench-scale systems operated with dairy manure (Coats et al., 2016; Hanson et al., 2016; Wei et al., 2014). This parameter set produced the highest $f_{\rm PHBV}$ in a bench-scale factorial (Guho, 2010) and has since enriched for consortia with high specific VFA uptake and PHBV storage rates (0.14 to 0.26 mol_{C,VFA}/(g_{VSS}·h) and 0.10 to 0.19 mol_{C,PHBV}/(g_{VSS}·h), respectively) and PHBV storage capacity (up to 0.9 g_{PHBV}/g_{VSS}, though more typically 0.3 to 0.5 g_{PHBV}/g_{VSS}; Coats et al., 2016). This parameter set may not reflect the true optimum for the process; however, employing the same operational parameters at both the bench- and pilot-scale reduces their contribution to the performance difference between the two. This allows the effects of process scale up to be determined more directly.

One prominent operational deviation from the bench-scale enrichment reactor analogs was the lack of VFA loading control. The fermenter liquor in the enrichment reactor's feed was dosed at a constant volumetric fraction, with the OLR (0.52 \pm 0.07 gcod,VFA/(L·d)) being allowed to drift with fluctuations in VFA content. Despite this lack of control, the OLR magnitude and variability was consistent with tightly

 $^{^{\}rm b}$ The parameter estimate \pm the parameter's estimated standard error (Section 2.3)

^c The peak PHBV mass fraction observed during the assessment.

^d The 3HV mole fraction at the peak PHBV mass fraction observed during the assessment.

controlled bench-scale analogs (0.44 to 0.72 $g_{COD,VFA}/(L\cdot d)$) and 0.04 to 0.1 $g_{COD,VFA}/(L\cdot d)$, respectively; Coats et al., 2016; Hanson et al., 2016). The larger fermenter liquor fraction at pilot-scale offset the comparatively low C_{VFA} of the fermenter liquor; however, the OLR was lower than in other studies using waste feedstocks (0.77 to 4.7 $g_{COD,VFA}/(L\cdot d)$; Conca et al., 2020; Tamis et al., 2014, 2018; Valentino et al., 2018, 2019). While detrimental to the overall volumetric productivity, this reduced loading was necessitated by the fermenter liquor's high solids content and propensity to foam voluminously when aerated.

In addition to the *OLR*, the temperature, pH, and dissolved oxygen—all commonly controlled enrichment reactor process variables at the bench- and pilot-scale—were left uncontrolled. The temperature ranged from approximately 16 to 27 $^{\circ}$ C over the operational period. The pH was relatively stable (when monitored) during most of the enrichment reactor assessments (typically 8.3 to 8.9). The $C_{\rm DO}$ was generally in the "aerobic" range, dipping, as expected, during each feast phase (typically down to 2 to 3 mg_{O2}/L, though several excursions below 1 mg_{O2}/L were experienced).

While the enrichment reactor's success is ultimately measured by the performance of its associated production reactor, its individual behavior—in particular its exhibition of the characteristic feast-famine response, adherence to key operational metrics, and overall consistency—provide predictors of overall process success. After an initial stabilization period, the enrichment reactor exhibited the characteristic feast-famine response (Fig. 2a): Following substrate addition, the $C_{\rm DO}$ was depressed while VFAs were consumed and PHBV synthesized. Once VFAs were exhausted, the $C_{\rm DO}$ increased, PHBV and NH $_3$ were consumed, and $C_{\rm X}$ increased.

Several metrics have been proposed as predictive or descriptive

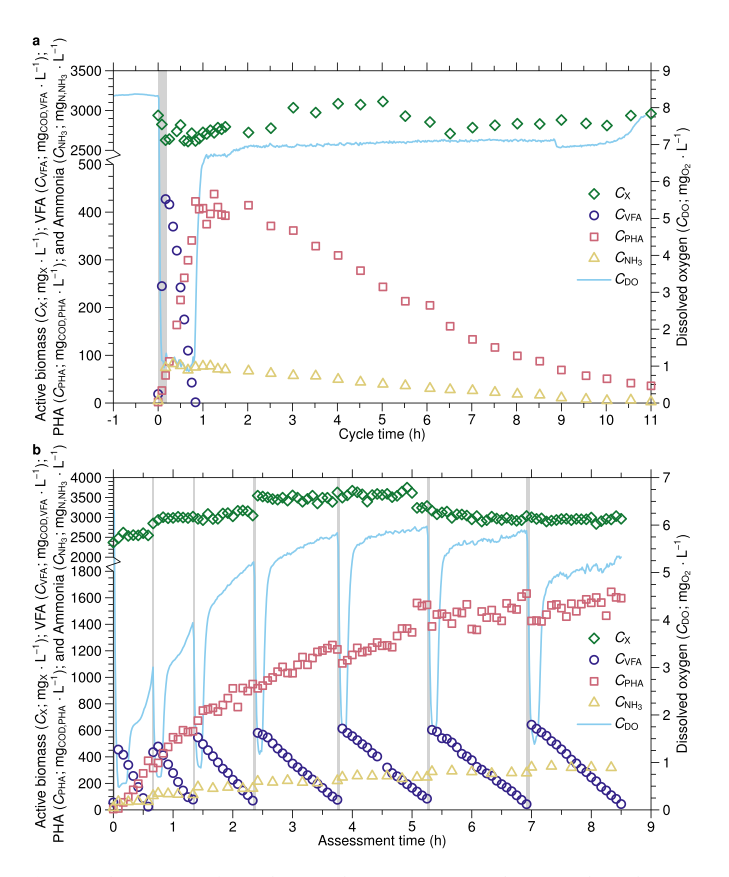


Fig. 2. Observations from the enrichment reactor cycle (**a**) and production reactor (**b**) assessments on a representative operational day (84), including the active biomass, volatile fatty acid, polyhydroxyalkanoate, ammonia, and dissolved oxygen concentrations ($C_{\rm X}$, $C_{\rm VFA}$, $C_{\rm PHBV}$, $C_{\rm NH3}$, and $C_{\rm DO}$, respectively). The gray regions denote the fill phase (the first 12 min of the cycle; **a**) and pulse additions (**b**). Note the break and scale change in the left ordinates.

measures of an enrichment reactor's effectiveness at enriching for PHA producing bacteria. They include the (i) number of cycles per SRT (fewer is better; Jiang et al., 2011); (ii) volume exchange ratio (larger is better; Marang et al., 2016); and (iii) ratio of feast to famine durations (the "feast-to-famine ratio"; Dionisi et al., 2006) and variations thereon (e.g., the feast-duration-to-CL ratio; Dionisi et al., 2006; Valentino et al., 2014, 2017). While the number of cycles per SRT (4.0) and the volume exchange ratio (0.25) herein fell outside the ranges reported in the metrics' originating and related studies (1.2 to 2 and 0.5 to 0.83, respectively; Jiang et al., 2011; Marang et al., 2016; Tamis et al., 2014, 2018), they were consistent with other pilot-scale systems (4 to 24 and 0.25 to 0.67, respectively; Morgan-Sagastume et al., 2014; Valentino et al., 2018, 2019). Both the feast-to-famine and feast-duration-to-CL ratios observed herein (0.034 \pm 0.004 and 0.033 \pm 0.004, respectively) were well below the oft-cited 0.2 maximum (Dionisi et al., 2006; Valentino et al., 2014, 2017). Together with the low end-of-cycle f_{PHBV} (0.00042 to 0.013 g_{PHA} / gcs), all of the metrics support the conclusion that a robust feast-famine metabolic response was elicited.

Given the less stringent operational control, the consistency of the enrichment reactor's performance is particularly noteworthy. While the feast length was monitored only intermittently during the first 28 days of operation, it stabilized to 48 ± 6 min (n = 60) after approximately 24 d (6 *SRTs*; see Fig. 1b). C_X and the peak f_{PHBV} were also consistent following stabilization (2.5 ± 0.2 g_X/L and 0.10 ± 0.01 g_{PHA}/g_{CS}, respectively; Table 1). Stabilization of the feast length, C_X , and peak f_{PHBV} after an initial acclimation period are commonly observed behaviors in feast-famine enrichment reactors (Johnson et al., 2010; Tamis et al., 2014).

In addition to these core metrics, the observed stoichiometric and kinetic variables of the enrichment reactor were also generally consistent, with the mean $q_{\rm VFA}^{\rm max}$ and $Y_{\rm PHBV,VFA}^{\rm of}$ for the 14 assessments following stabilization being $0.30\pm0.07~g_{\rm COD,VFA}/(g_{\rm X}\cdot h)$ and $0.8\pm0.1~g_{\rm COD,PHA}/g_{\rm COD,VFA}$, respectively (Table 1). These variables also closely aligned with those reported previously for bench-scale analogs (Coats et al., 2016), further supporting the resiliency of the process despite deviations in operation. More broadly, both variables were generally within the ranges reported for comparable pilot-scale systems (0.23 to 7.8 g_{COD,VFA}/(g_{\rm X}\cdot h) and 0.30 to 0.74 g_{COD,PHA}/g_{COD,VFA} for $q_{\rm VFA}^{\rm max}$ and $Y_{\rm PHBV,VFA}^{\rm post}$, respectively; Conca et al., 2020; Tamis et al., 2014, 2018; Valentino et al., 2018, 2019).

Importantly, not every facet of the enrichment reactor's performance was stable. The sludge volume index (SVI_{30}) varied from 75 to 310 mL/g over the operational period. While kinetic selection theory predicts a well-settling biomass in feast-famine PHBV systems, many have exhibited elevated and variable SVI_{30} s (Tamis et al., 2014, 2018). The variability observed herein was likely due, at least in part, to the lack of a selective pressure exerted on settling (with the SRT = HRT, no benefit is conferred by settling well). Past 16S rRNA gene sequencing work on bench-scale analogs has shown the MMCs enriched therein to be dominated by Meganema, a genus of filamentous bacteria (Coats et al., 2016; Hanson et al., 2016). Overproduction of hydrophobic extracellular polysaccharides, a trait of some PHA-producing bacteria (Huang et al., 2018), is an alternative (or possibly compounding) explanation. Regardless of its root cause, the poor settling will need to be remedied as a part of future scale up efforts.

3.3. Production Reactor

In keeping with the less stringent process control exerted over the preceding stages, production assessments were conducted under the simple fed-batch regime with manually-triggered, $C_{\rm DO}$ -based pulse addition and a floating *OLR*. The temperature, pH, and dissolved oxygen were also not controlled, ranging from approximately 17 to 26 °C, 8.2 to 9.1, and 0.20 to 8.0 mg_{O2}/L, respectively. The expected PHA storage dynamics were observed in each assessment (Fig. 2b): after each fermenter liquor pulse addition (i) VFAs were consumed; (ii) PHBV was

stored; and (iii) $C_{\rm DO}$ dropped and remained depressed until VFA depletion. Following stabilization, 5 to 7 pulses of fermenter liquor were added in each production assessment. The resulting durations (5 to 8.5 h; Table 3) were generally consistent with other pilot scale facilities (4 to 24 h; Tamis et al., 2014, 2018; Valentino et al., 2018).

By monitoring the $C_{\rm DO}$, the operator was able to dose the next pulse or end the assessment in a narrow window bracketing VFA depletion; excluding the first assessment and one lapse on operational day 78, the largest deviations were approximately 13 min before and 7 min after depletion. While a premature pulse addition may push $C_{\rm VFA}$ into inhibitory levels, the highest $C_{\rm VFA}$ encountered (26 mmol $_{\rm C,VFA}/{\rm L}$) was well below the $C_{\rm VFA}$ where inhibition has been observed (exceeding 60 mmol $_{\rm C,VFA}/{\rm L}$; Serafim et al., 2004). Moreover, the peak $C_{\rm VFA}$ during each production pulse was within 84 mg $_{\rm COD,VFA}/{\rm L}$ of the peak observed during the feast phase of the corresponding enrichment reactor assessment (mean of the 42 pulses constituting the seven stable assessments; the maximum deviation was 220 mg $_{\rm COD,VFA}/{\rm L}$). A late pulse addition, in contrast, may lead to inefficient performance if the MMC shifts to polymer consumption; however, the $C_{\rm VFA}$ and $C_{\rm PHBV}$ dynamics revealed no such penalty.

Considering the kinetic and stoichiometric variables, both the specific VFA uptake and PHA synthesis rates decreased with production assessment duration (Fig. 2b). $q^{\text{max}}_{\text{VFA}}$ estimates during the first pulse were comparable with those in the corresponding enrichment assessments but fell in subsequent pulses, typically stabilizing at 0.1 to 0.2 g_{COD,VFA}/(g_X·h) by the third pulse. The specific rate of PHA synthesis exhibited a similar reduction after the first pulses, but the behavior was less consistent. As a result, the Y^{obs}_{PHBV,VFA} varied between pulses as well, ranging from 0.24 to 1.4 g_{COD,PHBV}/g_{COD,VFA}. The cumulative observed yield (0.58 to 0.87 g_{COD,PHBV}/g_{COD,VFA} after stabilization; Table 3) was on the high end of values reported in other pilot scale facilities (0.4 to 0.64 g_{COD,PHBV}/g_{COD,VFA}; Conca et al., 2020; Tamis et al., 2018; Valentino et al., 2018). The elevated yields observed herein suggest PHA synthesis from non-VFA substrate (Hanson et al., 2016). In contrast, the volumetric productivity (0.11 to 0.18 g_{PHBV}/(L·h) after stabilization; Table 3), was lower than reported elsewhere (0.2 to 0.5 gpHA/(L·h); Conca et al., 2020; Valentino et al., 2018; Tamis et al., 2014). As is discussed in Section 3.6, this was due in large part to the low C_{VFA} of the fermenter liquor.

3.4. Characterizing PHA Synthase Genes in the MMC

Coupling molecular analysis of PHA biosynthesis with analytical chemistry investigations can elucidate potentially important relationships that may provide insight into the feast-famine metabolic response and facilitate future process scale-up. Work herein focused on the diversity and relative abundance of PHA synthase genes (*phaC*) in the MMC. *phaC* is critical in PHA synthesis, in that the associated enzyme polymerizes 3-hydroxyalkyl-CoAs to form PHA (Steinbüchel and Hein, 2001). To date, four classes of *phaC* have been identified: classes I, III, and IV polymerize short-chain-length (SCL; C3–C5) monomers, whereas class II polymerizes medium-chain-length (MCL; C6–C14) monomers (Ciesielski et al., 2008; Sheu et al., 2000).

Investigations first evaluated the potential presence of all four *phaC* gene classes in the pilot-scale MMC. Gel electrophoresis of the PCR-amplified genomic DNA revealed that the MMC contained *phaC* classes I and II, but not classes III or IV (Fig. S1). The presence of *phaC* class II is surprising, given that the PHA synthesized by the MMC was limited to SCL monomers (3HB and 3HV were the only monomers detected by GC–MS and ¹H NMR). While MCL monomer production by MMCs fed short-chain-length VFAs (which dominated the VFAs quantified in the fermenter liquor, Fig. 1a) has been reported (in particular 3-hydroxy-2-methylvalerate; Serafim et al., 2008), the behavior is not universal. MMCs enriched in bench-scale systems operated independent of but complementary to the pilot system studied herein have also consistently produced SCL PHA, with *phaC* class II genes detected (data not shown).

The lack of MCL monomers in each system suggests that the class II *phaC* genes detected were not actively transcribed but, instead suggest unrealized potential for more diverse polymer production. The detection of *phaC* class II genes in independent PHBV systems further suggests that this potential was not limited to the MMC enriched in one operational run, indicating unrealized MCL PHA production potential worthy of future exploration. Collectively these results align well with PHBV productivity potential associated with the C2–C6 VFA-rich substrate.

Relative abundance analysis of the phaC gene revealed phaC class II gene presence at 2.3 \pm 1.1% (n = 12) over six operational days (58, 61, 67, 71, 78, and 84); melting curve analysis showed an amplification efficiency of 85%, which was deemed acceptable for quantitation. Conversely, while phaC class I showed a bright signal on the gel for all operational days evaluated (Fig. S1a), amplification efficiency was less than 35% and thus quantitative analyses were not performed (Section S1.1). The stark difference in amplification efficiencies between the two primer sets may be attributed to differing specificity. Whereas the phaC class II primers used in this study (I-179 L and I-179R) appear to be highly specific to the target gene, phaC class I primers (CF1-CR4) exhibit low specificity for the target gene with numerous degenerate base pairs (Ciesielski et al., 2008). Further optimization, leveraging results from recent microbial ecology investigations conducted on a similar matrix (Coats et al., 2016), will be necessary for subsequent investigations, in particular for phaC class I. Nevertheless, successful detection and quantitation of phaC in such a diverse MMC enriched on complex substrate (Coats et al., 2016) well-positions subsequent investigations focused on elucidating enhanced structural details on the MMC, as well as related functional evaluations that could contribute to new insight on the feast-famine metabolism.

3.5. Downstream processing and polymer characterization

After each production assessment, 3 to 7 kg of PHBV-rich biomass was recovered (15 to $22\%_{TS}$) from which PHBV was extracted and purified. The yield of crude PHBV recovered from the PHBV-rich biomass was 21 to 32% (mass of crude PHBV per mass of PHBV-rich biomass, ash-free biomass basis) and the yield of purified PHBV from the PHBV-rich biomass was 17 to 28% (mass of purified PHBV per mass of PHBV-rich biomass; ash-free biomass basis). The purified PHBV was 82 to $97\%_{PHBV}$. In total, $65\pm18\%$ of the PHBV in the PHBV-rich biomass was recovered in the purified PHBV following extraction and purification. This purity and overall recovery efficiency are comparable with results obtained by others employing similar workflows for 3HB produced using pure cultures (e.g., 94 to 96% pure 3HB and 65 to 70% recovery; Ramsay et al., 1994).

The molar 3-hydroxyvalerate (3HV) content in the purified PHBV samples and PHBV standard was determined by ^1H NMR spectroscopy (Table 2 and Figs. S3 to S5). Chemical shifts were observed at the same resonance frequencies in the samples and standard (the triplet CH₃-proton in 3HV monomer at $\delta=0.94,0.92,$ and 0.89 ppm and the doublet CH₃-proton in the 3HB monomer at $\delta=1.31$ and 1.29 ppm; Wei et al., 2014). The resulting 3HV molar ratios (0.1 to 0.24 mol $_{3\text{HV}}$ /mol $_{p\text{HBV}}$) were in the range for PHBV biosynthesized from fermented dairy manure (Wei et al., 2014).

The molar mass (weight and number average) of purified PHBV samples was determined by SEC-MALS (Table 2). The $\overline{M_{\rm w}}$ were between 6.49 \times 10⁵ to 2.80 \times 10⁶ g/mol and comparable to those obtained by Wei et al. (2014) for PHBV produced in a bench-scale three-stage PHBV system fed dairy manure. The molar-mass dispersity ($D_{\rm M}$) of the lower $\overline{M_{\rm w}}$ PHBV samples (operational days between 32 and 84) were low (between 1.06 and 1.14). While, the high $\overline{M_{\rm w}}$ PHBV (operational day 15) had a higher $D_{\rm M}$ of 1.43 showing a broad molar mass range. These $D_{\rm M}$ values were lower than those reported by Wei et al. (2014) at around 2.2.

The thermal properties (glass transition temperature, T_g ; melting

Table 2 Purified PHBV material properties. a,b

Operational day	Purity % (g/g)	$f_{ m 3HV,PHBV}$		Molar mass			Thermal properties			
		GC-MS mol/mol	¹ H NMR mol/mol	$\overline{M_{\rm w}} \cdot 10^5$ g/mol	$\overline{M_{\rm n}} \cdot 10^5$ g/mol	$D_{ m M}$	T _g °C	T _{m1} °C	T _{m2} °C	<i>X_c</i> °C
15	82 ± 2	0.15 ± 0.02	0.16 ± 0.02	28 ± 1	19.6 ± 0.5	1.43 ± 0.04	-2.8 ± 0.3	126.3 ± 0.4	152.6 ± 0.2	25 ± 4
32	93 ± 2	0.18 ± 0.01	0.18 ± 0.01	8.7 ± 0.3	8.0 ± 0.3	1.09 ± 0.06	-6.1 ± 0.4	151.2 ± 0.5	166.6 ± 0.3	17.4 ± 0.2
39	94 ± 3	0.18 ± 0.01	0.19 ± 0.01	7.0 ± 0.4	6.4 ± 0.3	1.08 ± 0.08	-6.8 ± 0.9	159.8 ± 0.2	170.2 ± 0.2	23.2 ± 0.2
46	94 ± 4	0.23 ± 0.02	0.23 ± 0.01	8.5 ± 0.2	7.4 ± 0.1	1.15 ± 0.03	-8.8 ± 0.9	154.1 ± 0.3	165.4 ± 0.2	19.7 ± 1.2
61	94 ± 4	0.24 ± 0.01	0.24 ± 0.01	6.5 ± 0.2	6.0 ± 0.2	1.08 ± 0.05	-10 ± 1	146.7 ± 0.6	162.8 ± 0.3	18.7 ± 0.2
71	89 ± 1	0.23 ± 0.01	0.23 ± 0.01	6.9 ± 0.5	6.4 ± 0.4	1.07 ± 0.10	-6.3 ± 0.5	127.8 ± 0.8	156.7 ± 0.1	13.9 ± 1.6
78	95 ± 3	0.23 ± 0.01	0.22 ± 0.01	8.4 ± 0.2	8.0 ± 0.2	1.06 ± 0.03	-5.0 ± 0.8	128.1 ± 0.3	152.2 ± 0.5	19.7 ± 1.1
84	97 ± 2	0.21 ± 0.01	0.21 ± 0.01	11.3 ± 0.2	10.1 ± 0.2	1.12 ± 0.03	-6.0 ± 0.6	130.9 ± 0.1	153.5 ± 0.8	23.9 ± 0.6

^a Symbols are defined as: $f_{3\text{HV,PHBV}}$ is the fraction of 3 HV in PHBV; $\overline{M_w}$ is the weight-average molar mass; $\overline{M_n}$ is the number-average molar mass; D_M is the molar-mass dispersity $(D_M = \overline{M_w}/\overline{M_n})$; T_g is the glass transition temperature; T_{m1} and T_{m2} are temperature of the first and second melting peaks, respectively; and X_c is the degree of crystallinity. Purity is the mass of PHBV per unit mass of the purified PHBV expressed as a percentage.

temperature, $T_{\rm m}$; and degree of crystallization, $X_{\rm c}$) of the purified and standard PHBV were determined by DSC (Table 2 and Fig. S6) for setting processing (e.g., extrusion) conditions. All the PHBV samples showed a subambient $T_{\rm g}$ (-9.5 to -2.8 °C) consistent with that of the standard (-4.9 ± 0.1 °C). In general, $T_{\rm g}$ was found to decrease with increasing 3HV content, further reinforcing that the flexibility of the PHBV bioplastic ($T_{\rm g}$) can be controlled by its composition (Modi et al., 2011; Wei and McDonald, 2015). Two melting temperatures were observed as a result of the isodimorphism of the semi-crystalline PHBV (Lv et al., 2016), with the first ($T_{\rm m1}$) ranging from 126 to 160 °C and the second ($T_{\rm m2}$) from 152 to 170 °C. Both melting temperatures were higher than the standard ($T_{\rm m1} = 126.1 \pm 1.9$ °C and $T_{\rm m2} = 152.0 \pm 0.6$ °C) and no correlation was observed between PHBV $T_{\rm m}$ and 3HV content. The $X_{\rm c}$ of

the purified PHBV (13.9 to 25%) was generally higher than the standard (14.9 \pm 2.6%) and generally decreased with increasing 3HV content. This decrease is attributed to 3HV units inhibiting the crystallization of 3HB due to hydrogen bonding, thus limiting the crystallization of 3HB (Modi et al., 2011). The $T_{\rm m}$ and $X_{\rm c}$ of the standard and PHBV samples, which influence the polymer's mechanical properties and processability (Wei et al., 2015), were higher than those previously reported for PHBV produced from fermented dairy manure (0.32 to 0.34 mol_{3HV}/mol_{PHBV}; $T_{\rm m}=147$ to 148 °C; $X_{\rm c}=1.9$ to 2.1%; Wei et al., 2014).

3.6. Overall performance and future prospects

Several metrics have been put forth to measure the performance of a

Table 3Overall performance summary of the individual production assessments.

Operational Pulses day added ^c	Duration ^b	PHBV-rich biomass			Volumetric productivity			Cumulative observed		
	added ^c	h	$f_{ m PHBV}$		$f_{ m 3HV,PHBV}$	Production	Enrichment	Fermenter	yield ^g	
			g/g_{TS}	g/g _{VS} mol/mol	mol/mol	only ^d g _{PHBV} /(L·h)	included ^e	included ^f	gcod,phbv/gcod,vfa	
							$g_{PHBV}/(L \cdot h)$	$g_{PHBV}/(L \cdot h)$		
15	3	2.3	0.11 ± 0.01	$\begin{array}{c} 0.14 \pm \\ 0.01 \end{array}$	0.13 ± 0.01	0.079	0.0023	0.0014	0.31	
32	5	5.0	$\begin{array}{c} \textbf{0.24} \pm \\ \textbf{0.01} \end{array}$	$\begin{array}{c} 0.29 \pm \\ 0.01 \end{array}$	$\begin{array}{c} 0.23 \; \pm \\ 0.01 \end{array}$	0.17	0.013	0.0063	0.66	
39	5	6.2	$\begin{array}{c} 0.28 \pm \\ 0.01 \end{array}$	$\begin{array}{c} 0.33 \pm \\ 0.01 \end{array}$	$\begin{array}{c} 0.25 \; \pm \\ 0.01 \end{array}$	0.12	0.012	0.0058	0.72	
46	5	5.0	$\begin{array}{c} 0.30\ \pm \\ 0.01 \end{array}$	$\begin{array}{c} \textbf{0.35} \pm \\ \textbf{0.01} \end{array}$	$\begin{array}{c} 0.26 \pm \\ 0.01 \end{array}$	0.13	0.0098	0.0051	0.87	
61	7	6.8	$\begin{array}{c} 0.30\ \pm \\ 0.01\end{array}$	$\begin{array}{c} 0.35 \; \pm \\ 0.01 \end{array}$	$\begin{array}{c} 0.28 \pm \\ 0.01 \end{array}$	0.14	0.017	0.0076	0.81	
71	7	5.6	$\begin{array}{c} 0.29 \pm \\ 0.01 \end{array}$	$\begin{array}{c} 0.37 \; \pm \\ 0.01 \end{array}$	$\begin{array}{c} 0.27 \pm \\ 0.01 \end{array}$	0.18	0.017	0.0079	0.70	
78	6	6.0	$\begin{array}{c} 0.28 \pm \\ 0.01 \end{array}$	$\begin{array}{c} 0.35 \pm \\ 0.01 \end{array}$	$\begin{array}{c} 0.25 \; \pm \\ 0.01 \end{array}$	0.16	0.016	0.0074	0.71	
84	7	8.5	$\begin{array}{c} 0.33 \; \pm \\ 0.01 \end{array}$	$\begin{array}{c} \textbf{0.40} \pm \\ \textbf{0.01} \end{array}$	$\begin{array}{c} 0.22 \pm \\ 0.01 \end{array}$	0.11	0.016	0.0071	0.58	

^a Symbols are defined as: f_{PHBV} is the fraction of PHBV in the biomass and $f_{3HV,PHBV}$ is the fraction of 3HV in PHBV.

 $^{^{}m b}$ Values are mean \pm standard deviation. Where necessary, the standard deviation has been rounded up to the mean's reported precision.

b The duration of the production assessment, from the start of the first pulse addition to the time of the $C_{\rm DO}$ spike after the last.

^c The number of fermenter liquor pulses added to the production reactor over the assessment.

^d Volumetric productivity considering just the production reactor. Estimated as the C_{PHBV} in the production reactor at the end of the assessment divided by its duration.

 $^{^{\}rm e}$ Volumetric productivity considering the enrichment and production reactors. Estimated as the $M_{\rm PHBV}$ in the production reactor at the end of the assessment divided the product of 24 h (the enrichment reactor's cycle length, which exceeded each of the production assessment durations) and the total volume of the enrichment and production reactors.

 $^{^{\}rm f}$ Volumetric productivity considering the fermenter, enrichment, and production reactors. Estimated as the $M_{\rm PHBV}$ in the production reactor at the end of the assessment divided the product of 24 h (the cycle length of the fermenter and enrichment reactor, which exceeded each of the production assessment durations) and the total operating volume of the system. Being that the pilot-scale fermenter was undersized Section 2.1.1, the total system volume was the sum of the enrichment and production reactor volumes and that of an appropriately scaled fermenter (one with the same operational parameters as that employed herein, but able to deliver the fermenter liquor volume consumed without queueing).

g Estimated as the M_{PHBV} in the production reactor at the end of the assessment divided by the total M_{VFA} added to the production reactor throughout the assessment.

PHBV synthesizing process overall, including the PHBV mass fraction in the PHBV-rich biomass, the volumetric productivity of the process as a whole, and the overall observed yield (Reis et al., 2011). Of the eight production assessments, five achieved $f_{\rm PHBV}$ of at least 0.35 $g_{\rm PHBV}/g_{\rm VS}$, with the highest being 0.40 \pm 0.01 $g_{\rm PHA}/g_{\rm VS}$ (Table 3). While these values are low compared to prior work with macronutrient limited feedstocks (e.g., 0.7 $g_{\rm PHA}/g_{\rm VSS}$; Tamis et al., 2014), they are on the threshold for commercial viability (Bengtsson et al., 2017). The process' future prospects are nevertheless promising as options are available to reduce the non-PHA biomass contributed by the residual solids in the fermenter liquor (Section 3.1).

The volumetric productivity can vary substantially depending on the stages included in its calculation Reis et al. (2011). Regardless of the basis, the values realized herein (Table 3) were at least an order of magnitude lower than those reported for pure cultures; however, they were more comparable with other mixed culture systems. When limited to the production reactor, the volumetric productivities herein (0.11 to 0.18 gpHa/(L·h)) were in the range of those previously reported (0.049 to 0.6 gpHa/(L·h); Reis et al., 2011; Tamis et al., 2014; Valentino et al., 2018). Including the enrichment reactor, however, pushed the volumetric productivities below those observed in comparable systems (0.0098 to 0.017 gpHa/(L·h) vs. 0.045 to 0.25 gpHa/(L·h); Dionisi et al., 2006; Valentino et al., 2018).

The observed yield of the system as a whole as well as those of the individual stages (Fig. 3) are informative when considering the overall efficiency as well as the limitations of each step. Following the approach of Bengtsson et al. (2008), the yield of the process overall (excluding PHBV-rich biomass recovery) was estimated at approximately 0.035 g_{PHBV}/g_{COD} . This value is on the low end of the range of overall yields reported for comparable systems (0.036 to 0.2 g_{PHA}/g_{COD} ; Tamis et al., 2014, 2018; Valentino et al., 2018).

Several issues contributed to the comparatively low volumetric productivity and overall observed yield: (i) the fermenter liquor was not strictly macronutrient limited, which curtailed production potential; (ii) the enrichment reactor's high *SRT*, long *CL*, and low *OLR* reduced the mass flow rate of enriched MMC to the production reactor; and (iii) the fermenter's low VFA yield necessitated a significantly larger system to balance demand. While little may be done for the first issue, prior work suggests that the latter two may be countered by operational changes.

While the findings detailed herein for the processes individually and as a whole suggest stable and consistent performance despite less rigorous operational control, these conclusions must be appropriately tempered by the relatively short duration of the operational period from which they were derived. This limitation is common in pilot-scale studies of three-stage PHA systems, with many reporting operations of comparable duration (42 to 129 d; Tamis et al., 2014, 2018; Valentino et al., 2018). More prolonged operations spanning multiple seasons—such as those undertaken by Valentino et al. (2019) and Conca et al. (2020)—are necessary to validate the conclusions drawn herein and further crystallize the economic potential of the process.

4. Conclusions

This work demonstrates the successful transition of PHBV synthesis using fermented dairy manure from prior bench-scale studies to pilot-scale. Despite less stringent operational control, each stage performed consistently over the operational period, producing an economically viable PHBV mass fraction and a purified polymer with consistent material properties. Detection of PHA synthase gene class II suggests unrealized potential for medium-chain-length monomers. The stage performance individually and in aggregate was also assessed and impediments to process scale up were identified. Taken together, these results bode well for future pilot- and full-scale investigations and reinforce the potential for PHBV production from waste feedstocks.

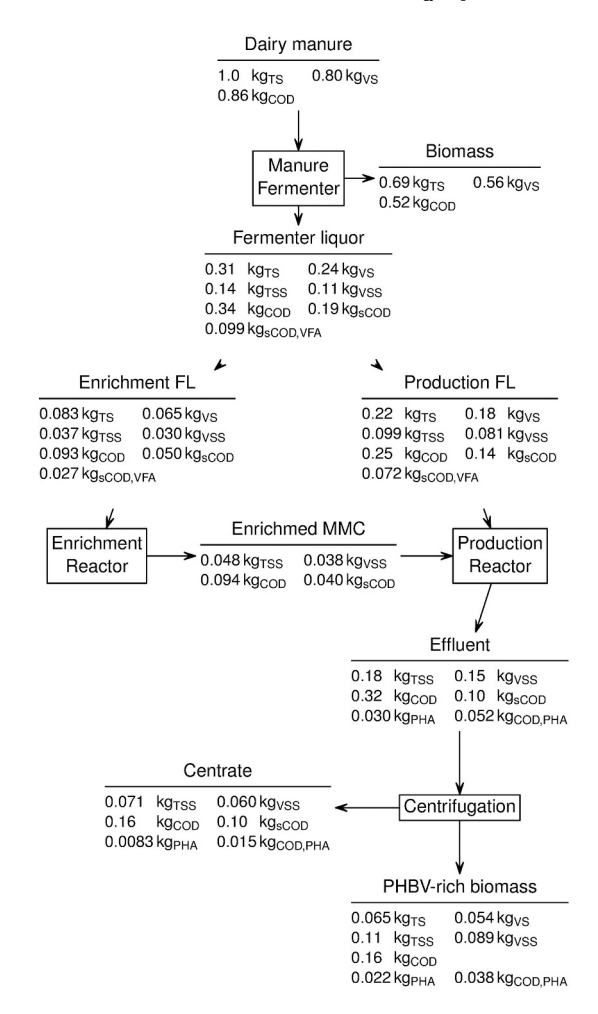


Fig. 3. Overall yield of the three stage PHBV production process from dairy manure normalized to 1 kg_{TS,manure}. Values reflect a reapportioned (balanced) system, rather than the system as implemented (Section 2.1.1). The fermenter and enrichment reactor yields reflect their mean behavior over the operational period. Due to the limited characterization of intermediate streams, the fermenter and fermenter liquor solids separation yields were aggregated. The production reactor and centrifuge yields reflect their mean performance following stabilization (i.e., the last seven production assessments; $Y_{\rm PHBV,VFA}^{\rm obs} = 0.53~{\rm gp_{HBV/g_{VFA}}}$ and $f_{\rm 3HV,PHBV} = 0.25~{\rm mol_{3HV}/mol_{PHBV}}$; Table 3). Total COD was not determined analytically. For manure, a value of of 1.08 $g_{\rm COD}/g_{\rm VS}$ was assumed (American Society of Agricultural and Biological Engineers, 2005). For subsequent streams, the total was taken as the sum of the soluble COD and the particulate COD, with the latter being estimated by 1.42 $g_{\rm COD}/g_{\rm VSS}$.

CRediT authorship contribution statement

Nicholas M. Guho: Conceptualization; Methodology; Validation; Formal analysis; Investigation; Writing

Dikshya Pokhrel, Maryam Abbasi, Maribel Alfaro, Cynthia K. Brinkman: Methodology; Formal analysis; Writing

Armando G. McDonald: Supervision; Writing

Erik R. Coats: Supervision; Project administration; Funding acquisition; Writing; Methodology; Conceptualization

Declaration of competing interest

The authors declare that they have no known competing financial interests or personal relationships that could have appeared to influence the work reported in this paper.

Acknowledgments

The material presented and discussed herein is based upon work supported by (i) the U.S. Department of Agriculture National Institute of Food and Agriculture under Grant Number 2018-67022-27894, (ii) the Idaho Global Entrepreneurial Mission (IGEM) Grant Number IGEM19-001, (iii) the National Science Foundation under Grant Number CBET-1705728, and (iv) the U.S. Department of Agriculture National Institute of Food and Agriculture Hatch program under Grant Number IDA01585. Additional support was provided by (i) the University of Idaho Equipment and Infrastructure Support (EIS) Awards Program from the Office of Research and Economic Development, University of Idaho (ORED) RISE Funding Program and the College of Natural Resources in the purchase of the GC–MS and (ii) USDA-CSREES grant 2007-34158-17640 in the purchase of the DSC. Any opinions, findings, and conclusions or recommendations expressed in this material are those of the authors and do not necessarily reflect the views of the funding agencies.

Appendix A. Supplementary data

Supplementary data to this article can be found online at https://doi.org/10.1016/j.biteb.2020.100588.

References

- American Society of Agricultural and Biological Engineers, 2005. Manure Production and Characteristics. American Society of Agricultural and Biological Engineers. ASAE D384.2 MAR2005 (R2019).
- Bengtsson, S., Werker, A., Christensson, M., Welander, T., 2008. Production of polyhydroxyalkanoates by activated sludge treating a paper mill wastewater. Bioresour. Technol. 99 (3), 509–516.
- Bengtsson, S., Werker, A., Visser, C., Korving, L., 2017. PHARIO: stepping stone to a sustainable value chain for PHA bioplastic using municipal activated sludge. STOWA. 2017-15.
- Berthet, M.-A., Gontard, N., Angellier-Coussy, H., 2015. Impact of fibre moisture content on the structure/mechanical properties relationships of PHBV/wheat straw fibres biocomposites. Compos. Sci. Technol. 117, 386–391.
- Ciesielski, S., Pokoj, T., Klimiuk, E., 2008. Molecular insight into activated sludge producing polyhydroxyalkanoates under aerobic-anaerobic conditions. J. Ind. Microbiol. Biotechnol. 35 (8), 805–814.
- Coats, E.R., Loge, F.J., Wolcott, M.P., Englund, K., McDonald, A.G., 2008. Production of natural fiber reinforced thermoplastic composites through the use of polyhydroxybutyrate-rich biomass. Bioresour. Technol. 99 (7), 2680–2686.
- Coats, E.R., Ibrahim, I., Briones, A., Brinkman, C.K., 2012. Methane production on thickened, pre-fermented manure. Bioresour. Technol. 107, 205–212.
- Coats, E.R., Watson, B.S., Brinkman, C.K., 2016. Polyhydroxyalkanoate synthesis by mixed microbial consortia cultured on fermented dairy manure: effect of aeration on process rates/yields and the associated microbial ecology. Water Res. 106, 26–40.
- Conca, V., da Ros, C., Valentino, F., Eusebi, A.L., Frison, N., Fatone, F., 2020. Long-term validation of polyhydroxyalkanoates production potential from the sidestream of municipal wastewater treatment plant at pilot scale. Chem. Eng. J. 390.
- Dias, J.A.M.L., Lemos, P.C., Serafim, L.S., Oliveira, C., Eiroa, M., Albuquerque, M.G.E., Ramos, A.M., Oliveira, R., Reis, M.A.M., 2006. Recent advances in polyhydroxyalkanoate production by mixed aerobic cultures: from the substrate to the final product. Macromol. Biosci. 6 (11), 885–906.
- Dionisi, D., Majone, M., Vallini, G., Di Gregorio, S., Beccari, M., 2006. Effect of the applied organic load rate on biodegradable polymer production by mixed microbial cultures in a sequencing batch reactor. Biotechnol. Bioeng. 93 (1), 76–88.
- Fernádez-Dacosta, C., Posada, J.A., Kleerebezem, R., Cuellar, M.C., Ramirez, A., 2015. Microbial community-based polyhydroxyalkanoates (PHAs) production from wastewater: Techno-economic analysis and ex-ante environmental assessment. Bioresour. Technol. 185, 368–377.
- Guho, N.M., 2010. Polyhydroxyalkanoate Production Coupled With Waste Treatment Using a Three-stage Sequencing Batch Reactor System Fed Dairy Manure (Unpublished master's Thesis). University of Idaho, Moscow, Idaho, USA.
- Gurieff, N., Lant, P., 2007. Comparative life cycle assessment and financial analysis of mixed culture polyhydroxyalkanoate production. Bioresour. Technol. 98 (17), 2202, 2402
- Hanson, A.J., Guho, N.M., Paszczynski, A.J., Coats, E.R., 2016. Community proteomics provides functional insight into polyhydroxyalkanoate production by a mixed microbial culture cultivated on fermented dairy manure. Appl. Microbiol. Biotechnol. 100 (18), 7957–7976.
- Huang, L., Chen, Z., Wen, Q., Zhao, L., Lee, D.-J., Yang, L., Wang, Y., 2018. Insights into feast-famine polyhydroxyalkanoate (PHA)-producer selection: Microbial community succession, relationships with system function and underlying driving forces. Water Res. 131, 167–176.

- Jiang, Y., Marang, L., Kleerebezem, R., Muyzer, G., van Loosdrecht, M.C.M., 2011. Effect of temperature and cycle length on microbial competition in PHB-producing sequencing batch reactor. ISME J. 5 (5), 896–907.
- Jiang, Y., Marang, L., Tamis, J., van Loosdrecht, M.C.M., Dijkman, H., Kleerebezem, R., 2012. Waste to resource: Converting paper mill wastewater to bioplastic. Water Res. 46 (17), 5517–5530.
- Johnson, K., Kleerebezem, R., van Loosdrecht, M.C.M., 2010. Influence of the C/N ratio on the performance of polyhydroxybutyrate (PHB) producing sequencing batch reactors at short SRTs. Water Res. 44 (7), 2141–2152.
- Korkakaki, E., van Loosdrecht, M.C.M., Kleerebezem, R., 2017. Impact of phosphate limitation on PHA production in a feast-famine process. Water Res. 126, 472–480.
- Luzier, W.D., 1992. Materials derived from biomass/biodegradable materials. Proc. Natl. Acad. Sci. U. S. A. 89 (3), 839–842.
- Lv, Y., Zhu, H., An, M.-f.; Xu, H.-j.; Zhang, L.; Wang, Z.-b., 2016. Multiple endothermic peaks resulted from different crystal structures in an isomorphous copolymer poly (3-hydroxybutyrate-co-3-hydroxyvalerate). Chin. J. Polym. Sci. 34 (12), 1510–1522.
- Madison, L.L., Huisman, G.W., 1999. Metabolic engineering of poly(3-hydroxyalkanoates): from DNA to plastic. Microbiol. Mol. Biol. Rev. 63 (1), 21–53.
- Majone, M., Massanisso, P., Carucci, A., Lindrea, K., Tandoi, V., 1996. Influence of storage on kinetic selection to control aerobic filamentous bulking. Water Sci. Technol. 34 (5–6), 223–232.
- Marang, L., van Loosdrecht, M.C.M., Kleerebezem, R., 2016. Combining the enrichment and accumulation step in non-axenic PHA production: cultivation of *Plasticicumulans* acidivorans at high volume exchange ratios. J. Biotechnol. 231, 260–267.
- Modi, S., Koelling, K., Vodovotz, Y., 2011. Assessment of PHB with varying hydroxyvalerate content for potential packaging applications. Eur. Polym. J. 47 (2), 179–186.
- Morgan-Sagastume, F., Valentino, F., Hjort, M., Cirne, D., Karabegovic, L., Gerardin, F., Johansson, P., Karlsson, A., Magnusson, P., Alexandersson, T., Bengtsson, S., Majone, M., Werker, A., 2014. Polyhydroxyalkanoate (PHA) production from sludge and municipal wastewater treatment. Water Sci. Technol. 69 (1), 177–184.
- Negulescu, I. I.; Cueto, R.; Wing, M. G.; Stevens, B.; Rusch, K.; and Jacobs, A., 2008. Size exclusion chromatography of bioderived poly(hydroxy alkanoate)s. Abstr. of Pap. of the Am. Chem. Soc., 236.
- Ramakers, C., Ruijter, J.M., Lekanne Deprez, R.H., Moorman, A.F.M., 2003. Assumption-free analysis of quantitative real-time polymerase chain reaction (PCR) data. Neurosci. Lett. 339 (1), 62–66.
- Ramsay, J.A., Berger, E., Voyer, R., Chavarie, C., Ramsay, B.A., 1994. Extraction of poly-3-hydroxybutyrate using chlorinated solvents. Biotechnol. Tech. 8 (8), 589–594.
- Reis, M., Albuquerque, M., Villano, M., Majone, M., 2011. Mixed culture processes for polyhydroxyalkanoate production from agro-industrial surplus/wastes as feedstocks. In: Moo-Young, M. (Ed.), Comprehensive Biotechnology, second ed. Pergamon, Oxford pp, pp. 669–683.
- Rice, E.W., Baird, R.B., Eaton, A.D., Clesceri, L.S. (Eds.), 2012. Standard Methods for the Examination of Water and Wastewater Twenty-second Ed. American Public Health Association, American Water Works Association, Water Environment Federation, Washington, D.C.
- Serafim, L.S., Lemos, P.C., Oliveira, R., Reis, M.A.M., 2004. Optimization of polyhydroxybutyrate production by mixed cultures submitted to aerobic dynamic feeding conditions. Biotechnol. Bioeng. 87 (2), 145–160.
- Serafim, L.S., Lemos, P.C., Albuquerque, M.G.E., Reis, M.A.M., 2008. Strategies for PHA production by mixed cultures and renewable waste materials. Appl. Microbiol. Biotechnol. 81 (4), 615–628.
- Shen, L., Worrell, E., Patel, M., 2010. Present and future development in plastics from biomass. Biofuel Bioprod. Biorefining: Biofpr 4 (1), 25–40.
- Sheu, D.-S., Wang, Y.-T., Lee, C.-Y., 2000. Rapid detection of polyhydroxyalkanoateaccumulating bacteria isolated from the environment by colony PCR. Microbiol. 146 (8), 2019–2025.
- Steinbüchel, A., Hein, S., 2001. Biochemical and molecular basis of microbial synthesis of polyhydroxyalkanoates in microorganisms. In: Steinbüchel, A. (Ed.), Babel, W. Advances in Biochemical Engineering/Biotechnology. Springer, Berlin, pp. 81–123.
- Stowe, E.J., Coats, E.R., Brinkman, C.K., 2015. Dairy manure resource recovery utilizing two-stage anaerobic digestion — implications of solids fractionation. Bioresour. Technol. 198, 237–245.
- Sudesh, K., Abe, H., Doi, Y., 2000. Synthesis, structure and properties of polyhydroxyalkanoates: biological polyesters. Prog. Polym. Sci. 25 (10), 1503–1555.
- Tamis, J., Lužkov, K., Jiang, Y., van Loosdrecht, M.C.M., Kleerebezem, R., 2014. Enrichment of *Plasticicumulans acidivorans* at pilot-scale for PHA production on industrial wastewater. J. Biotechnol. 192 (A), 161–169.
- Tamis, J.; Mulders, M.; Dijkman, H.; Rozendal, R.; van Loosdrecht, M. C. M.; and Kleerebezem, R., 2018. Pilot-scale polyhydroxyalkanoate production from paper mill wastewater: process characteristics and identification of bottlenecks for full-scale implementation. J. Environ. Eng., 144(10).
- Valentino, F., Beccari, M., Fraraccio, S., Zanaroli, G., Majone, M., 2014. Feed frequency in a sequencing batch reactor strongly affects the production of polyhydroxyalkanoates (PHAs) from volatile fatty acids. New Biotechnol. 31 (4), 264-275.
- Valentino, F., Morgan-Sagastume, F., Campanari, S., Villano, M., Werker, A., Majone, M., 2017. Carbon recovery from wastewater through bioconversion into biodegradable polymers. New Biotechnol. 37 (A), 9–23.
- Valentino, F., Gottardo, M., Micolucci, F., Pavan, P., Bolzonella, D., Rossetti, S., Majone, M., 2018. Organic fraction of municipal solid waste recovery by conversion into added-value polyhydroxyalkanoates and biogas. ACS Sustain. Chem. Eng. 6 (12), 16375–16385.
- Valentino, F., Moretto, G., Lorini, L., Bolzonella, D., Pavan, P., Majone, M., 2019. Pilotscale polyhydroxyalkanoate production from combined treatment of organic fraction

- of municipal solid waste and sewage sludge. Ind. Eng. Chem. Res. 58 (27), 12149–12158.
- van Loosdrecht, M.C.M., Pot, M.A., Heijnen, J.J., 1997. Importance of bacterial storage
- polymers in bioprocesses. Water Sci. Technol. 35 (1), 41-47.
 Wei, L. and McDonald, A. G., 2015. Peroxide induced cross-linking by reactive melt processing of two biopolyesters: poly(3-hydroxybutyrate) and poly(L-lactic acid) to improve their melting processability. J. Appl. Polym. Sci., 132(13).
- Wei, L.; Guho, N. M.; Coats, E. R.; and McDonald, A. G., 2014. Characterization of poly(3hydroxybutyrate-co-3-hydroxyvalerate) biosynthesized by mixed microbial consortia fed fermented dairy manure. J. Appl. Polym. Sci., 131(11).
- Wei, L., McDonald, A.G., Stark, N.M., 2015. Grafting of bacterial polyhydroxybutyrate (PHB) onto cellulose via in situ reactive extrusion with dicumyl peroxide. Biomacromolecules 16 (3), 1040-1049.
- Winkler, M., Coats, E.R., Brinkman, C.K., 2011. Advancing post-anoxic denitrification for biological nutrient removal. Water Res. 45 (18), 6119–6130.